Supplemental Information

Linker Dependent Bond Rupture Force Measurements in Single-Molecule Junctions

M. Frei[1], S Aradhya[1], M. S. Hybertsen[2], L. Venkataraman[1]

[1]Department of Applied Physics and Applied Mathematics,
Columbia University, New York, NY 10027.
[2]Center for Functional Nanomaterials,
Brookhaven National Labs, Upton, NY 11973

Email: mhyberts@bnl.gov; lv2117@columbia.edu

Contents:

1. Experimental Details

Experimental Setup and Procedures: The conductive AFM consists of a modified AFM head (Multimode Veeco), external adder and filter circuits (SRS), as well as a homebuilt cantilever holder. A bias was applied between a gold coated, conductive cantilever (TAP300 BudgetSensors) and an Au substrate placed on top of a single-axis piezoelectric positioner with built-in position sensor (Mad City Labs). The resulting current was converted to a voltage with a current amplifier (Keithley 428). Data collection and control of the piezoelectric positioner were done by means of a data acquisition board (National Instruments, PXI-4461) driven by a customized program using Igor software (Wavemetrics Inc.). For the simultaneous conductance and force trace measurements, the substrate approached the cantilever tip until a set conductance larger than $5G_0$ was measured to ensure that the Au/molecule/Au junction from the previous measurement was completely destroyed. For standard conductance and force measurements, the sample was withdrawn at a rate of 18 nm/s and the current and force versus position data was recorded at a sampling frequency of 100 kHz. All position determinations were based on measurements with a built-in position sensor within our custom piezoelectric positioner. This position sensor was calibrated both by the manufacturer and by us using laser interference measurements. We found the absolute values of the measured displacements to be accurate to within 5%.

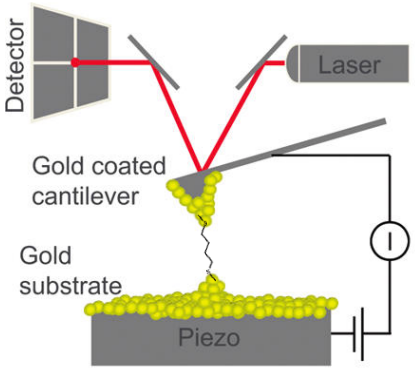

SI Figure S1*: Schematic of the AFM measurement set-up.*

Cantilever Calibration details: Force resolution along the pulling direction is achieved by measuring the deflection of a focused laser that is reflected off the back of a cantilever using a quadrant detector. The voltage signal corresponding to the deflection of the laser is converted to force in two steps. First the

quadrant detector signal is converted to a deflection in nm by forcing a solid contact between the sample substrate and the cantilever and subsequently moving the substrate by a known distance using the piezo. Second, the spring constant of the cantilever is determined using the power spectrum method[1]. The voltage signal in nm is converted to a force by multiplying by the cantilever spring constant. The determined Au-Au breaking force which is consistent with accepted values from literature[2], validates our calibration method.

2. Data Analysis

Conductance Step Detection: The molecular junction conductance step detection was carried out as follows. First, 1D conductance histograms were computed from all measured traces for each molecule to determine the conductance peak location and its width. This determines a minimum and maximal conductance value for each of the molecules studied. For each measured trace, the number of data points within this conductance range is determined. If this number of points is larger than the number required for a 0.02 nm plateau, the plateau length and slope, normalized to the average conductance are obtained. Traces with a conductance plateau longer than 0.02 nm and with a normalized slope larger than -5, are selected for further analysis. For each selected trace, the end of the conductance plateau is determined, and the conductance trace is analyzed to ensure that there was a sharp conductance drop following this plateau. This is done by requiring that the conductance after the plateau was less than 0.2 times that of the plateau (irrespective of the molecule type). 2D conductance and force histograms were then generated from all selected traces.

2D Histograms: Each measured conductance and force trace consisted of data acquired every 10 μs, measured at a constant 18 nm/s velocity. As conductance plateaus occur in random locations along the entire displacement axis (x-axis) within the measured range for each trace, we first set the origin of our displacement axis at the point where either the $1G_0$ conductance step or the molecular conductance step breaks. This well-defined position on the x-axis is determined individually for each trace, using an automated algorithm as described above. Each data point on the digitized conductance (force) trace now has a conductance (force) coordinate (along the y-axis) and a position coordinate (along the x-axis). Two dimensional conductance histograms are then generated without further analysis. For the two-dimensional force histogram, we also set the force at the zero-displacement position to zero force by subtracting an offset from the entire force trace. This realigns all force traces to a common point such that each force and displacement value is now determined relative to that at the end of the conductance step in each trace. After this re-alignment, thousands of force traces are added to generate a two-dimensional force

histogram. A statistically averaged force profile is obtained from this histogram from the peak of a Gaussian that is fit to vertical sections at every displacement bin.

Force Based Event Recognition Algorithm: In force based event recognition all events are identified using force data. The goal is to determine the location of every sharp force event occurring in each trace. This is achieved using a three step algorithm: (1) we subtract, from the raw force trace, a smoothed and laterally offset force trace. This effectively highlights low frequency changes of the force signal. (2) We multiply these by the square of the derivative of the original force trace. (3) The resulting trace ('Analyzed Force' in SI Figure S2) has sharp spikes at locations where the original force trace has sharp drops. These sharp spikes that are larger than a cut-off are selected. The cutoff is chosen to be 20 times the standard deviation of the Analyzed Force trace which ensures that selected spikes are significantly larger than small deviations in the Analyzed Force due to measurement noise. SI Figure S2 shows a sample conductance (red) and force (blue) trace that has been analyzed in this manner. It also shows, in black, the Analyzed Force trace where all drops are identified for gold point contact. For each measurement, the location of each spike along with the force and conductance right before and right after is recorded. For illustration, in the example of breaking a single-atom gold point contact, the conductance before the identified force event would be close to the quantum of conductance (G_0) and that right after would be below G_0.

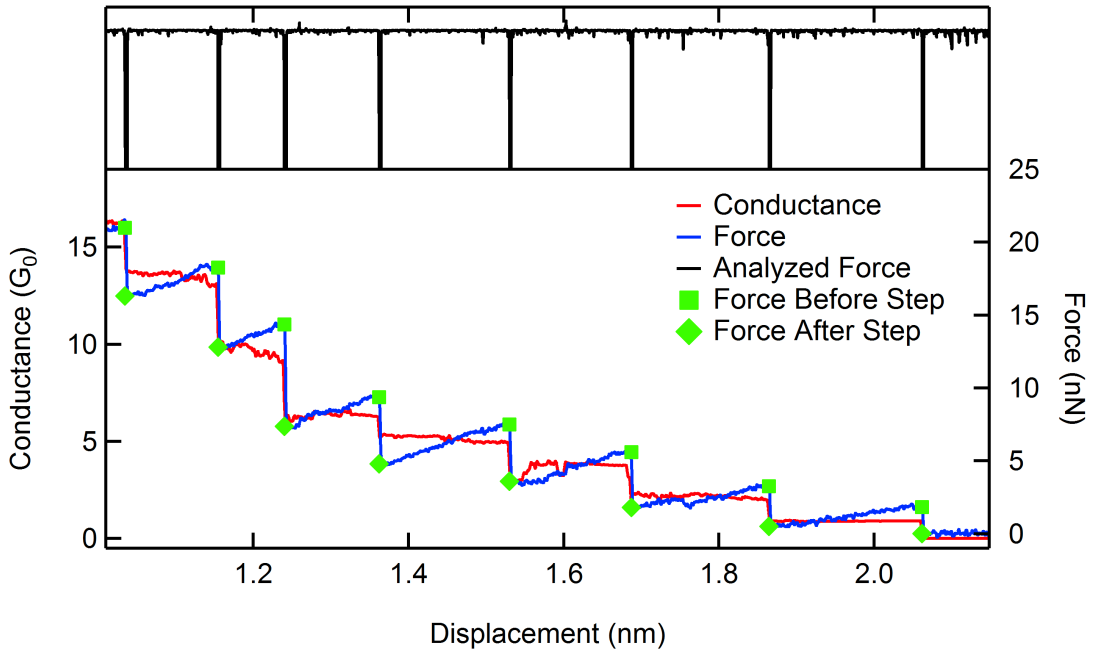

SI *Figure S2:* *Force based event recognition illustrated for a gold point contact. The analyzed force trace (black) effectively highlights the force events, and the multi-fit procedure accurately determines the force before (green square) and after (green diamond).*

Force traces are further analyzed to make sure that each event identified exhibits a well-defined saw-tooth signature. For a given force event, we fit three-line segment around the rupture location as shown in SI Figure S3. We select the fit with the lowest error from 400 different fit combinations where the end of line segment one (X1) and beginning of line segment 3 (X2) are varied in 20 incremental steps of 0.0006 nm along the displacement axis. This iterative fitting mechanism is more accurate in determining the location of rupture events which are often not correctly identified within a distance of 0.004 nm. In order to further eliminate fitting inaccuracies we also exclude traces for which the end of the first line segment (X1) occurs after the start of the third line segment (X2) and traces for which the middle segment has a positive slope (SI Figure S3). Finally the numerical value of each rupture is taken as the difference between the value of fit at X1 and X2.

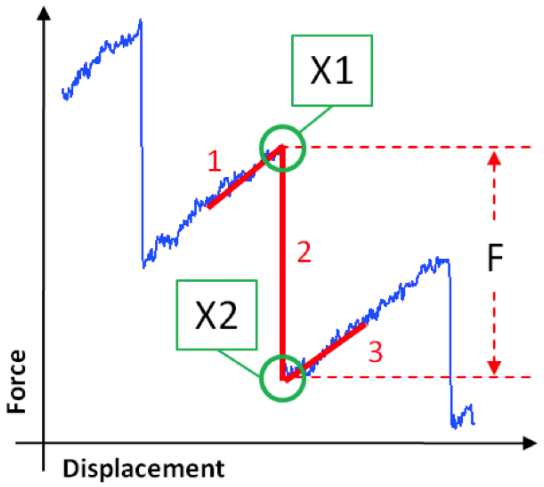

SI Figure S3: *A schematic of the force based event recognition fitting procedure. 400 three segment lines (1,2,3) are fit to the force event by varying X1 and X2 incrementally and the one with the smallest error is chosen.*

Histograms of rupture forces are generated. A Gaussian fit is used to determine a most likely breaking force for the particular bond breaking under consideration. By comparison with our conductance based event identification method, we find good agreement for the average rupture force. The main limitation to this method is that small force events are hard to reliably distinguish from the background noise. From our conductance based analysis, we have found that small force events are statistically meaningful when evaluating the average breaking force. Therefore, the purely force-based method may overestimate the average breaking force.

Additional Data:

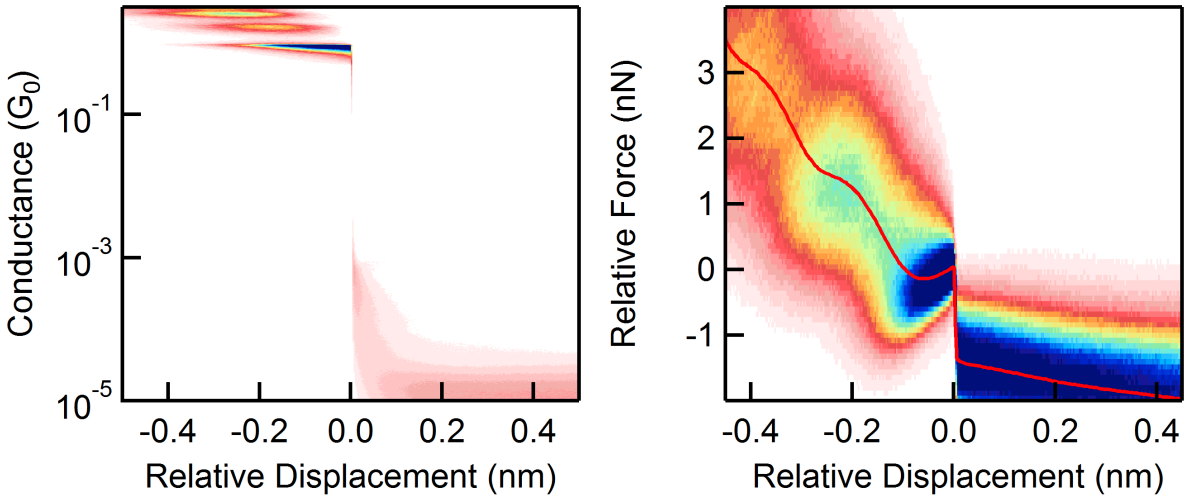

SI Figure S4: ***(A)*** *2D conductance histogram (15542 traces) for clean gold traces showing quantized steps above* $1G_0$ *and a clean break to experimental noise.* ***(B)*** *2D force histogram for the simultaneously measured force traces showing the force profile in red indicating a most probable breaking force for the gold-gold bond of 1.4 nN.*

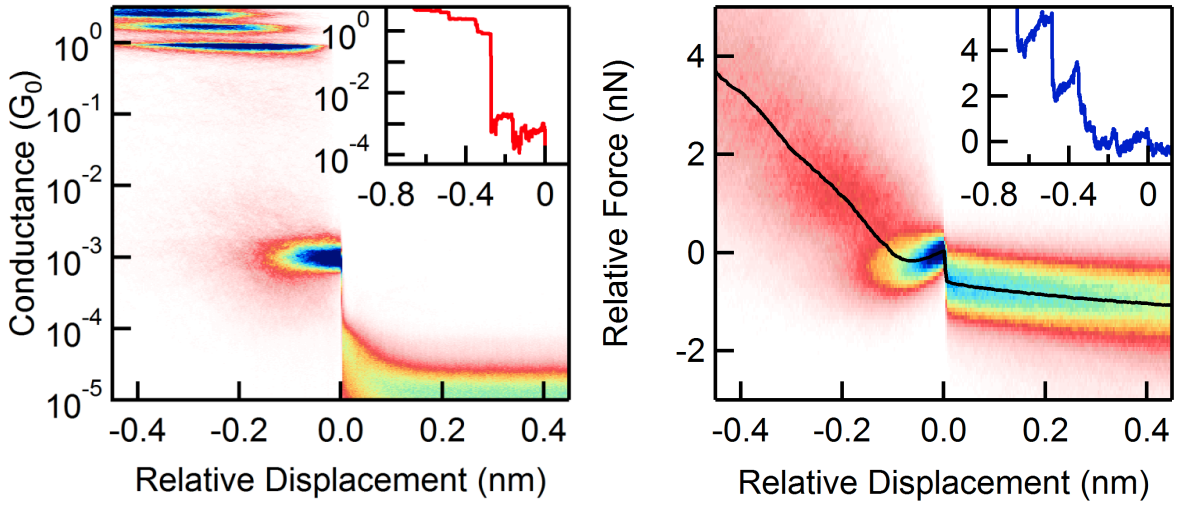

SI Figure S5: ***(A)*** *2D conductance histogram (3544 traces) for* $C4NH_2$ *showing quantized steps above* $1G_0$ *and a typical molecular signature at around* 10^{-3} G_0*. Inset: sample conductance trace* ***(B)*** *2D force histogram for the simultaneously measured force traces. The average force profile (black) indicates a breaking force of 0.6 nN. Inset: sample force trace.*

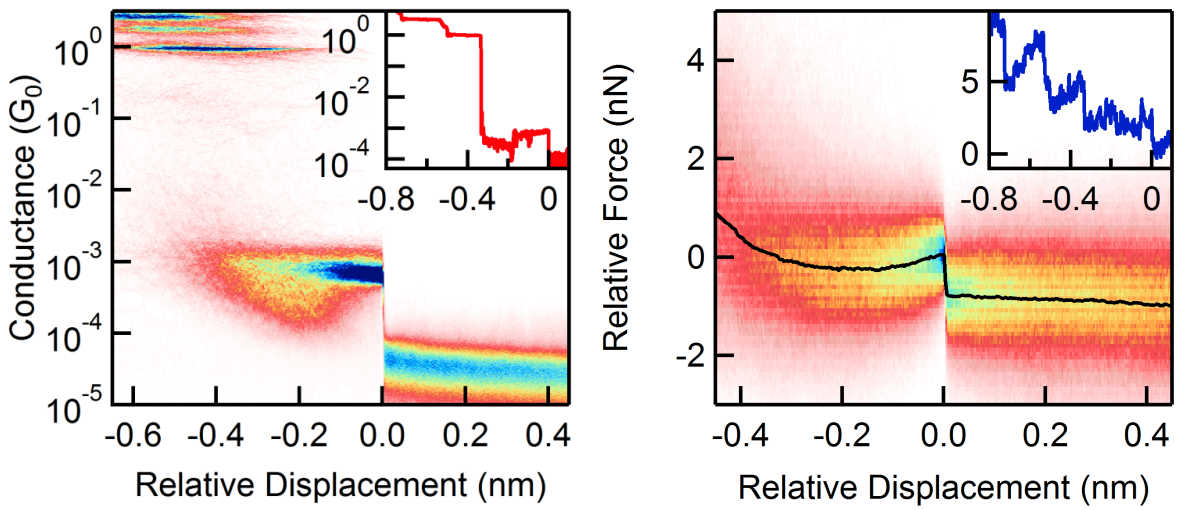

SI Figure S6: (A) *2D conductance histogram (1694 traces) for C5DPP showing quantized steps above* $1G_0$ *and a typical molecular signature for C5DPP at around* 6.6×10^{-4} G_0. *Inset: sample conductance trace.* ***(B)*** *2D force histogram for the simultaneously measured force traces. The average force profile (black) indicates a breaking force of 0.8 nN. Inset: sample force trace*

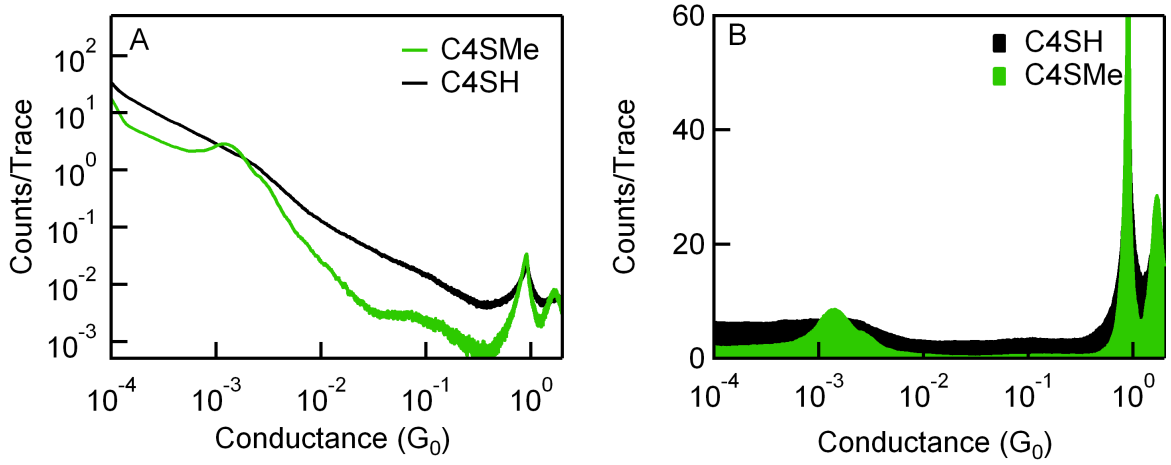

SI Figure S7. *One dimensional conductance histograms for C4SMe (green, 10000 traces) and C4SH (black, 14000 traces).* ***(A)*** *Histograms created using linear bins of size 0.00001* G_0. ***(B)*** *Log-binned histograms created using 100 bins per decade.*

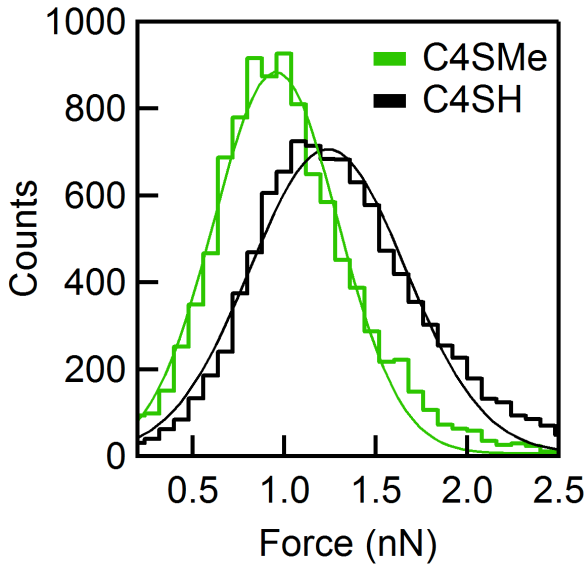

SI Figure S8: *Histograms of maximum force events per trace with conductance values consistent with molecular features for C4SMe (green, 10092 events, peak at 0.9 nN) and C4SH (black, 22888 events, peak at 1.2 nN).*

4. Procedures for Theoretical Calculations and Results

We use density functional theory (DFT) based calculations to simulate the junction elongation and rupture process for several links studied here, following the procedure outlined[3]. Briefly, the Au tip and surface were modeled with Au pyramids (20 atoms each) with (111) surfaces. The tip atom on the top pyramid was moved to an adatom site on one facet resulting in a blunt, three atom tip. The junction was elongated from near a local energy minimum through the inflection point and finally probed the dissociated structure after one bond ruptures. The back layer of Au atoms in each pyramid was held fixed with a bulk lattice parameter 4.08 Å. All other degrees of freedom were relaxed until all forces were less than 0.005-0.01 eV/Å for each junction structure. The junction was elongated in steps of 0.1 Å by increasing the separation between the pyramids along the z direction and then fully optimizing the geometry. Density functional theory total energy calculations and geometry optimization were performed with the VASP package[4], using the projector augmented wave approach which naturally included scalar relativistic effects for gold[5,6] and the generalized gradient approximation (GGA) of Perdew, Burke and Ernzerhof

(PBE)[7] for the exchange-correlation density functional. The model junction was placed in a hexagonal supercell (a=2.0nm, c=3.5nm) and the basis set for solution of the Kohn-Sham equations was determined by a 400 eV cutoff. The total energy and applied force computed from adiabatic junction elongation trajectories for each C4SMe is shown in SI Figure S9. A simplified structure was used to compare maximum sustained force between SMe and SH by focusing on half of the junction (Figure S10). In these simulations, an ethane with a single link group bonded to a single tip is studied by systematically moving the molecule upwards relative to the tip, holding the vertical position of the S atom fixed.

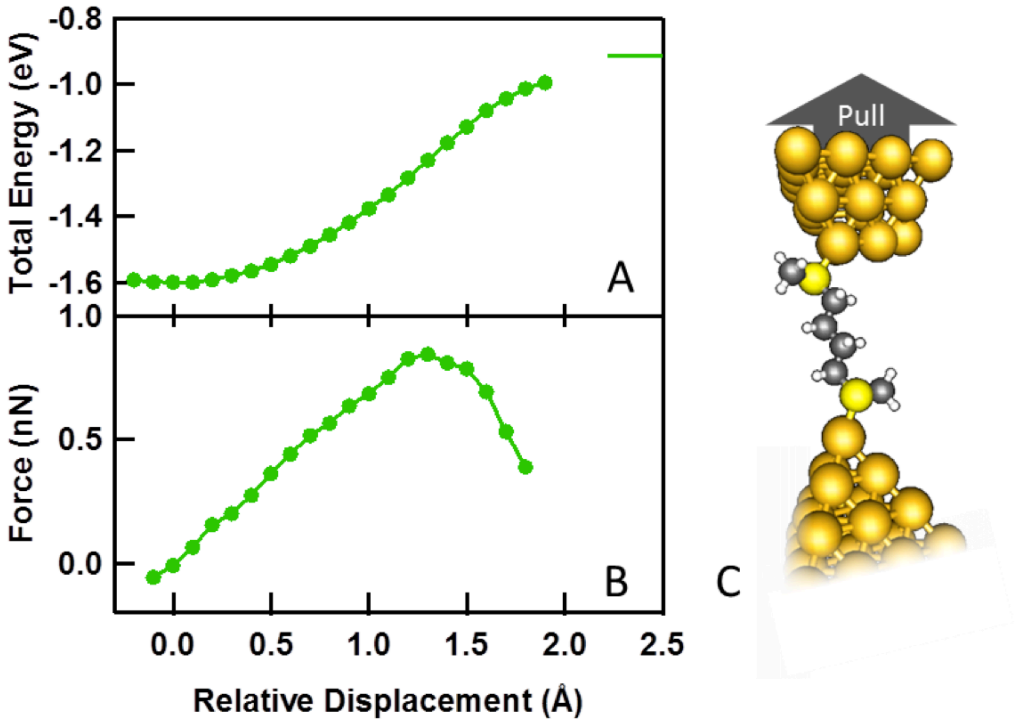

SI Figure S9: ***(A)*** *Calculated total energy curve from an adiabatic trajectory for C4SMe shown as a function of displacement. Bar shown at right indicates the asymptotic value.* ***(B)*** *Calculated applied force curve for the same molecule shown against displacement.* ***(C)*** *C4SMe junction structure for displacement near the local energy minimum.*

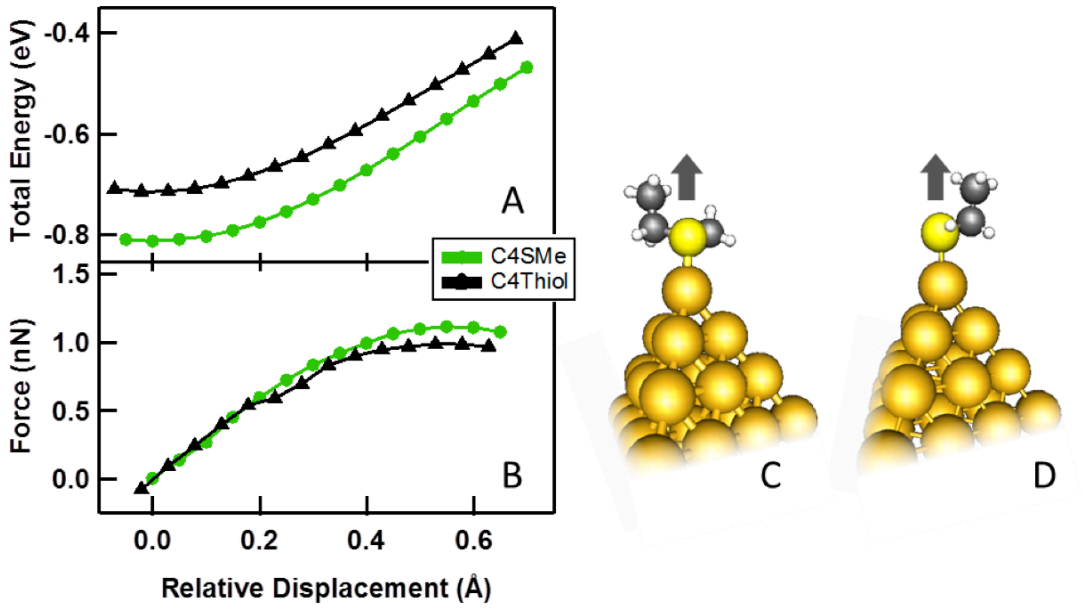

SI Figure S10: (A) *Calculated total energy and* ***(B)*** *force curves from a one-sided junction structure* ***(C and D)*** *comparing the SMe and SH donor-acceptor bond rupture forces. Initial geometry as illustrated in* ***(C)*** *and* ***(D)****, with the bond aligned to vertical. Displacement is controlled by fixing the position of the back plane of Au atoms in the cluster modeling the electrode and the S atom bonded to the Au tip atom.*

Finally, similar studies were performed for ethanethiolate model structures bonded to 21 atom gold tips (Figure S11). An initial structure was designed to probe the maximum sustainable force under ideal conditions of near vertical elongation along the S-Au bond, with the Au link atom bonded to three Au atoms in the next layer. The upper C atom and one of the C-H bonds is held fixed to maintain backbone orientation and overall elongation. This structure sustains 1.9 nN before substantial plastic rearrangement of the tip structure. The second structure explores the rupture process when the Au link atom is minimally coordinated, being bonded to a single Au atom on the tip. In this example, there is minimal shear force on the tip and the structure ruptures at the Au-Au bond with a maximum sustained force of less than 1.4 nN. This is somewhat smaller than the typical Au-Au rupture force in gold point contact DFT simulations (1.6 nN) [8,9]. Trajectories with larger shear force on the tip structure resulted in plastic deformation of these small model tip structures.

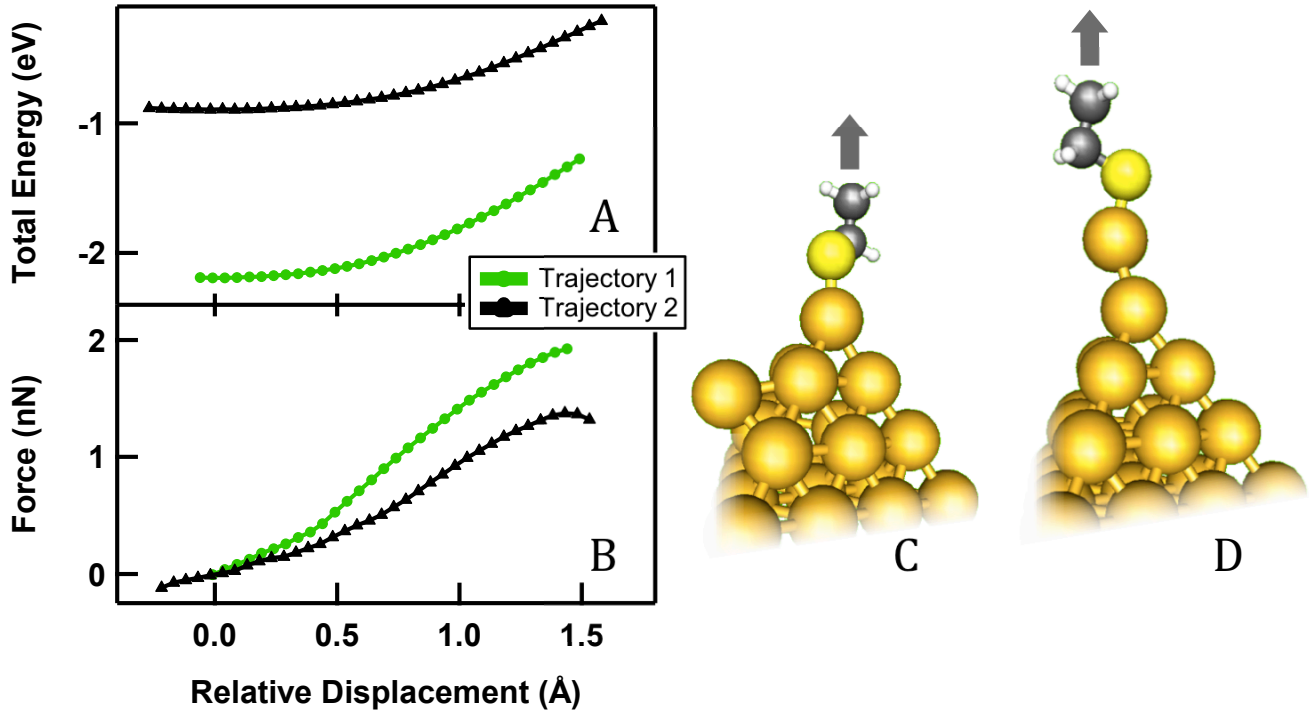

SI Figure S11: ***(A)*** *Calculated total energy and* ***(B)*** *force curves from a one-sided junction structure* ***(C*** *and* ***D)*** *comparing two thiolate elongation scenarios. Initial geometry as illustrated in* ***(C)*** *and* ***(D)****. Displacement is controlled by fixing the position of the back plane of Au atoms in the cluster modeling the electrode and the upper C atom as well as the C-H bond aligned to the ethane backbone. The reference tip structure for (C) has an Au atom on the side of the tip while for (D) the tip structure after rupture is the ideal pyramid.*

5. References

[1] J. L. Hutter and J. Bechhoefer, "Calibration of atomic-force microscope tips", *Review of Scientific Instruments* **64**, 1868-1873 (1993).

[2] G. Rubio, N. Agrait, and S. Vieira, "Atomic-sized metallic contacts: Mechanical properties and electronic transport", *Phys. Rev. Lett.* **76**, 2302-2305 (1996).

[3] M. Frei, S. V. Aradhya, M. Koentopp, M. S. Hybertsen, and L. Venkataraman, "Mechanics and Chemistry: Single Molecule Bond Rupture Forces Correlate with Molecular Backbone Structure", *Nano Lett.* **11**, 1518-1523 (2011).

[4] G. Kresse and J. Furthmuller, "Efficient iterative schemes for *ab initio* total-energy calculations using a plane-wave basis set", *Phys. Rev. B* **54**, 11169 (1996).

[5] G. Kresse and D. Joubert, "From ultrasoft pseudopotentials to the projector augmented-wave method", *Phys. Rev. B* **59**, 1758-1775 (1999).
[6] P. E. Blochl, "Projector Augmented-Wave Method", *Phys. Rev. B* **50**, 17953-17979 (1994).
[7] J. P. Perdew, K. Burke, and M. Ernzerhof, "Generalized gradient approximation made simple", *Phys. Rev. Lett.* **77**, 3865-3868 (1996).
[8] G. Rubio-Bollinger, S. R. Bahn, N. Agrait, K. W. Jacobsen, and S. Vieira, "Mechanical properties and formation mechanisms of a wire of single gold atoms", *Phys. Rev. Lett.* **8702**, 026101 (2001).
[9] Y. Qi, J. Qin, G. Zhang, and T. Zhang, "Breaking Mechanism of Single Molecular Junctions Formed by Octanedithiol Molecules and Au Electrodes", *Journal of the American Chemical Society* **131**, 16418-16422 (2009).